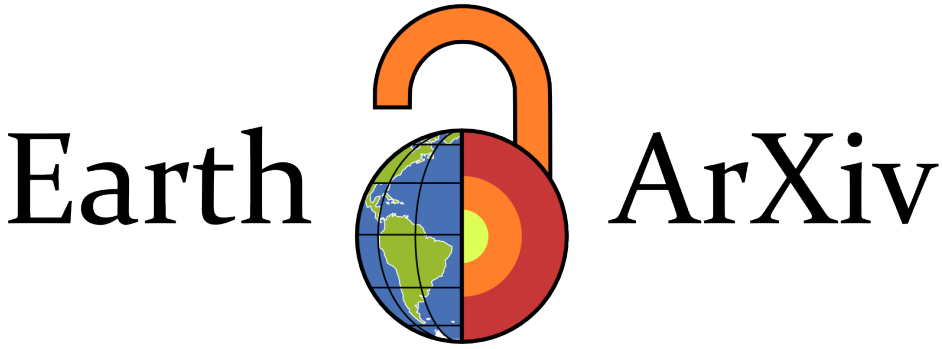

Peer review status:

This is a non-peer-reviewed preprint submitted to *Atmospheric Research* (December 2025).

Seasonal Wind Turbine-Associated Lightning in Central Europe

M. Kákona[a,b,c], R. Duspara[d], Z. Sokol[e], J. Popová[e], J. Chum[e], J. Šlegl[a,f], M. Sommer[a], M. Lužová[a,f], R. Dvořák[a], V. Hanousek[g], J. Kákona[a,h], A. Kostinsky[a], I. Ambrožová[a], O. Ploc[a]

[a]*Nuclear Physics Institute of the CAS, Husinec-Řež 130, Řež, 25068, Czech Republic*
[b]*Institute of Experimental Physics SAS, Watsonova 47, Košice, 04001, Slovakia*
[c]*Lawrence Berkeley National Laboratory, 1 Cyclotron Road, Berkeley, CA, 94720, USA*
[d]*Czech Thunderstorm Research Association, Prague, Czech Republic*
[e]*Institute of Atmospheric Physics of the CAS, Boční II 1401/1a, Prague, 14100, Czech Republic*
[f]*Faculty of Nuclear Sciences and Physical Engineering, Czech Technical University in Prague, Břehová 7, Prague, 11000, Czech Republic*
[g]*Institute of Information Theory and Automation of the CAS, Pod Vodárenskou věží 1143/4, Prague, 18200, Czech Republic*
[h]*Faculty of Electrical Engineering, Czech Technical University in Prague, Technická 2, Prague, 16627, Czech Republic*

Abstract

We report systematic evidence that cold-season lightning in Central Europe frequently occurs in close proximity to wind turbines. Using Blitzortung stroke data (2021–2024), ENTLN data (2023), and electric field measurements, we identify a recurring phenomenon - Seasonal Wind Turbine-Associated Lightning (SWAL), characterised by strokes clustering within proximity of wind turbines and exhibiting exclusively negative polarity. Electric field observations show strong negative near-ground fields, suggesting that the lower positive charge layer is weak or absent and that the main negative charge region becomes exposed. These results raise the broader question of whether SWAL would occur in landscapes without wind turbines, or whether such episodes would otherwise fail to develop into fully formed winter thunderstorms.

Keywords: Lightning, Wind turbines, Winter lightning, Blitzortung, ENTLN, Electric field mill

1. Terminology and Definitions

Lightning science spans multiple measurement domains (optical, radio, electrostatic, current sensing,...), each using partly overlapping terminology. Commonly used terms such as *flash*, *stroke*, *strike*, or *lightning* do not necessarily refer to the same physical phenomenon. To ensure clarity and reproducibility, we explicitly define the terminology adopted in this study. Definitions follow the operational criteria used in our analysis and may differ from conventions used in other subfields.

1.1. Lightning Stroke

The lightning channel current can be written as

$$I(t) = I_{\text{slow}}(t) + I_{\text{fast}}(t),$$

where the slow component represents quasi-steady current and the fast component represents rapid impulsive changes (e.g., return strokes, recoil leaders).

Loop antennas used in lightning detection systems do not measure the current directly. A voltage (electromotive force, EMF) is induced at the antenna terminals according to Faraday's law in response to the time derivative of the magnetic field produced by the lightning channel. The induced EMF $\mathcal{E}(t)$ may be approximated as

$$\mathcal{E}(t) = -M_{\text{eff}} \frac{dI_{\text{fast}}}{dt},$$

where M_{eff} is the effective mutual inductance between the lightning channel and the antenna. This mutual inductance depends on the distance and relative orientation between the channel and the loop, on the geometry of the current path, and on the frequency-dependent response of both the antenna and the front-end electronics.

Because $I_{\text{slow}}(t)$ varies only on time scales much longer than the antenna bandwidth, its contribution to dI/dt and therefore to the induced EMF is negligible. The measured voltage predominantly reflects the fast impulsive component of the lightning current, and provides a distorted band-limited estimate of dI_{fast}/dt.

For the purposes of this study, we define a *Lightning Stroke* as any detected EMF peak, irrespective of whether it corresponds to a return stroke, recoil leader, or another fast impulsive process during a lightning.

1.2. Lightning Event or simple Event

A Lightning Event represents the full electromagnetic activity associated with a lightning phenomenon over a short interval of time. In this study, a Lightning Event is defined as a contiguous sequence of lightning strokes with a total duration of up to 1 s. This threshold is motivated by the median lightning-event duration of approximately 0.5 s reported in Kákona et al. (2023). Rare cases of substantially longer events may occur, but their frequency is sufficiently low that they do not affect the statistical conclusions of this work.

Because a term with a similar meaning, flash, is typically used in optical detection systems, we avoid that terminology and use Lightning Event consistently for radio-derived temporal clusters of strokes.

1.3. Lightning Episode

In this study, we use the term *Lightning Episode* to describe a meteorological situation that might traditionally be referred to as a "thunderstorm". Because our analysis focuses on the cold season, we avoid presuming that such episodes exhibit the characteristics of summertime-like thunderstorms.

A Lightning Episode is therefore defined as a cluster of Lightning Events that were radio-detected within the study area, typically occurring within a single calendar day. This terminology captures the meteorological context of winter lightning without implying the presence of a fully developed thunderstorm.

1.4. Lightning Strike

A stroke classified by the lightning detection network as a cloud-to-ground (CG) lightning discharge is labeled as a *Strike*. A single Lightning Event may contain multiple strikes. In this study, we do not distinguish between downward and upward strikes, as such discrimination is beyond the resolution and capability of the detection systems used.

1.5. Limitations of Stroke Localization

Radio-based lightning locating systems estimate source points corresponding to strong dI/dt, which do not necessarily coincide with:

- maxima of the lightning current,
- maxima of dI/dt,

- physical CG attachment points.

This results from uncertainties inherent to Time Difference of Arrival (TDoA) or Direction Finding (DF) methods, the frequency response of the receiving antennas, and the fact that all reported stroke locations represent a two-dimensional projection of a three-dimensional discharge process. Furthermore, while a physical lightning stroke is an extended channel segment, lightning location networks operationally reduce this complex structure to a single point-like source location. Throughout this paper, the term "Stroke" therefore refers exclusively to this radio-detected source point reported by the lightning detection network, not to the full spatial extent of the underlying discharge.

2. Introduction

Lightning strikes pose a significant hazard to wind turbines (Candela Garolera et al., 2016), particularly during winter (Montanyà et al., 2016). Japanese coastal regions document that up to 95% of turbine strikes occur in the cold season (Matsui et al., 2020), but winter lightning in connection with wind turbines in inland continental Europe remains poorly understood.

Although some studies report changes in cloud-to-ground lightning statistics following the installation of wind farms (Chen et al., 2021), and several theories attempt to explain how wind turbines may initiate lightning discharges (Montanyà et al., 2014), the underlying mechanisms remain unresolved. Experimental data that would allow a complete understanding of the interaction between wind turbines and lightning remain limited.

Between 2018 and 2019, amateur observers from the Czech Thunderstorm Research Association noticed unusual winter lightning near wind farms in western Czechia and eastern Germany. These observations raised the question whether effects similar to those reported in other regions of the world may also occur in Central Europe. Since 2021, stroke-level data from the radio lightning detection network Blitzortung (Wanke, 2011) have enabled systematic investigation of this phenomenon.

Motivated by the unresolved questions outlined above, and enabled by the recent availability of Blitzortung data, the objectives of this study are to:

1. test whether cold-season lightning strokes occur with statistically significant proximity to wind turbines in Central Europe,

2. characterize their type and, in the case of strikes, their polarity,
3. analyze local electric field conditions during the cold season.

3. Methods

We analyze lightning strokes detected by radio detection networks from 2021 to 2024 and wind turbine positions obtained from OpenStreetMap (OSM) (OpenStreetMap contributors, 2024) as available in the 2024 dataset.

3.1. Extraction of Lightning Strokes

Lightning strokes were obtained from the Blitzortung VLF/LF network (Wanke, 2011), which locates radio sources associated with rapid changes in lightning channel current. Reported horizontal location accuracy is typically 1.4 km (Narita et al., 2018).

For further classification of lightning strokes, we used the ENTLN network (Mallick et al., 2015). Unlike Blitzortung, this network also provides information on the stroke altitude, and in the case of CG strikes (where the reported altitude is zero) it additionally provides the stroke polarity, which follows the standard physical definition (Rakov and Uman, 2003), i.e., the polarity corresponds to the sign of the net charge transferred to ground.

Although Blitzortung is a community-operated network, its spatial accuracy is sufficient for the statistical analyses performed here, and the results are cross-validated with ENTLN data where available.

3.2. Extraction of Wind Turbines and High-Rise Structures

Geographical positions of wind turbines and high-rise man-made structures were extracted from OSM using the Overpass Turbo API (Overpass API Developers, 2025). OSM data quality in Europe is more than adequate for this purpose, with typical horizontal accuracy on the order of 1.5 m (Haklay, 2010), which is negligible compared to the uncertainty of lightning location.

Wind turbine coordinates were obtained using the following query:

```
[out:json][timeout:150];
nwr["generator:source"="wind"] (49, 11, 51, 14);
out center;
```

High-rise structures other than wind turbines were obtained with:

```
[out:json][timeout:150];
(
    nwr(if:number(t["height"]) > 70) ["generator:source"!~"wind"]["man_made"](49,
    nwr(if:number(t["building:levels"]) > 25) (49, 11, 51, 14);
);
out center;
```

High-rise structures, in our study, are defined as man-made objects with a height exceeding 70 m above ground level or buildings with more than 25 floors. This includes skyscrapers, communication towers and masts, tall chimneys, cooling towers, and similar structures.

3.3. Study Area and Electric Field data

The study area (Fig. 1) is defined as a circle of radius 60 km centered at (50.26°N, 12.52°E), where Boltek EFM-100 electric field mill (Boltek Corporation, 2023) (EFM) is located. According to OSM (January 2025), this area contains 369 wind turbines and 47 other high-rise structures.

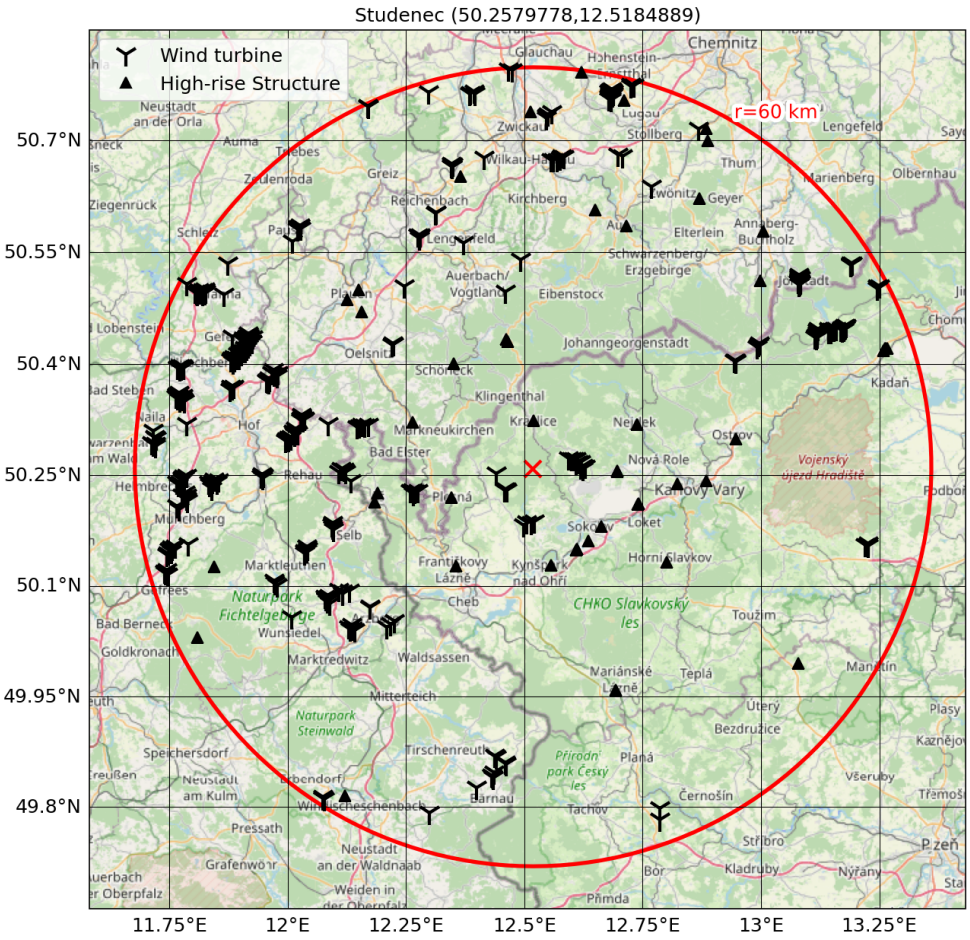

Figure 1: Map of the study area with the locations of wind turbines and high-rise structures within a 60 km radius. Map data © OpenStreetMap contributors, licensed under ODbL 1.0. The red cross mark in the center is the position of our EFM sensor.

3.4. Radar data

For radar analysis, we used the **ČHMÚ MAX3D** product, which represents the **maximum reflectivity in a vertical column** above each grid point. This composite reflectivity typically captures echo maxima located at altitudes of approximately **2–4 km** above mean sea level. MAX3D provides a robust indicator of the presence and motion of the main hydrometeor regions.

3.5. Distance Computation

Distances between each Blitzortung stroke and the nearest wind turbine or high-rise structure were computed using great-circle distances.

3.6. Reproducibility and Analysis Code

All analysis scripts, including statistical evaluation, are available at Kákona et al. (2025).

4. Results

4.1. Stroke distribution relative to ground objects

Because the spatial distribution of wind turbines and high-rise structures is inherently uneven, it is first necessary to characterise their statistical distribution across the landscape. To this end, we generated a synthetic dataset of 1000 strokes with a uniform spatial distribution and constructed the corresponding histogram (Fig. 2). This reference distribution provides a baseline that allows a meaningful comparison with the probability distribution of lightning events, both those unrelated to wind turbines and those observed during real lightning episodes.

An identical distance-to-object analysis applied to the real strokes from the 24 November 2023 snowstorm (Fig. 3), shows that more than 94.5% of the strokes occurred within 1.4 km of a wind turbine, whereas none were located within this distance of high-rise structures. Let us recall that a distance of 1.4 km corresponds to the reported location accuracy of the Blitzortung network. This episode is presented solely as an illustrative example intended to demonstrate the shift in the statistical distribution of strokes. It was selected because it generated lightning strokes throughout the full spatial extent of the study area.

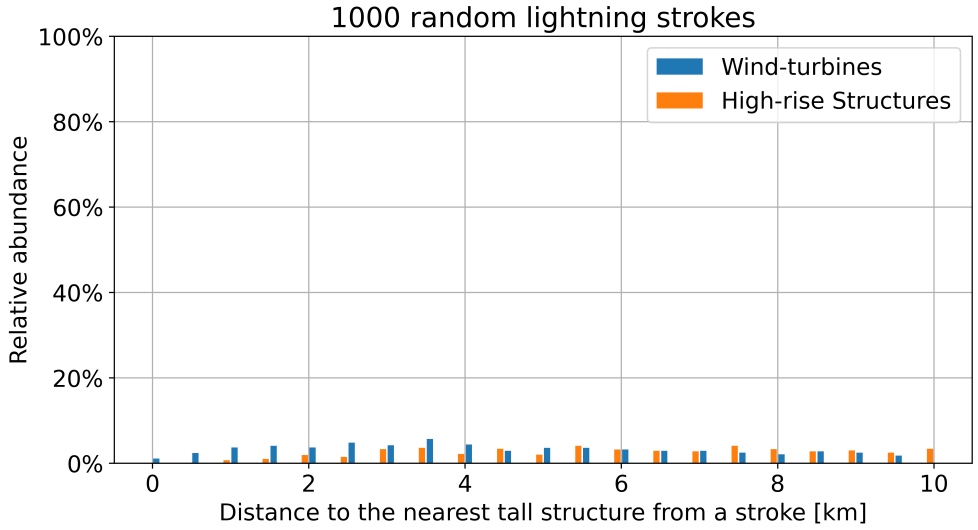

Figure 2: Histogram of distances to the nearest wind turbine (blue) and high-rise structure (orange) for 1000 randomly generated strokes within the study area.

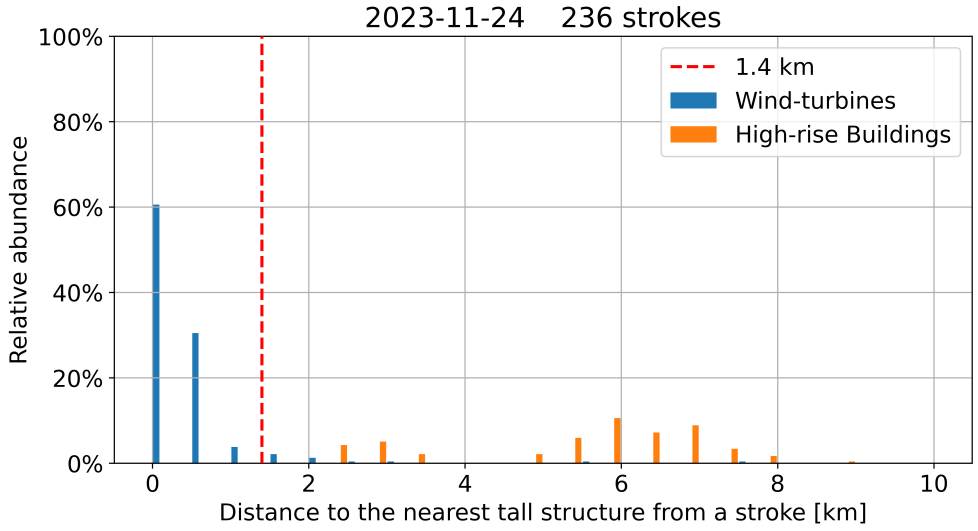

Figure 3: Histogram of distances to the nearest wind turbine (blue) and high-rise structure (orange) for 236 lightning strokes detected during the 24 November 2023 snowstorm. A total of 94.5% of all strokes (223 out of 236) occurred within 1.4 km of at least one wind turbine. None occurred within this distance of any other high-rise structure. The dashed line marks the estimated horizontal location uncertainty (≈1.4 km).

4.2. Temporal analysis

Fig. 4 shows days (lightning episodes) with at least one stroke. Circles' sizes correspond to stroke counts during one day; vertical position is the median distance to the nearest wind turbine. The median was chosen as the statistical metric because it is robust against small variations in the statistical distribution within individual episodes.

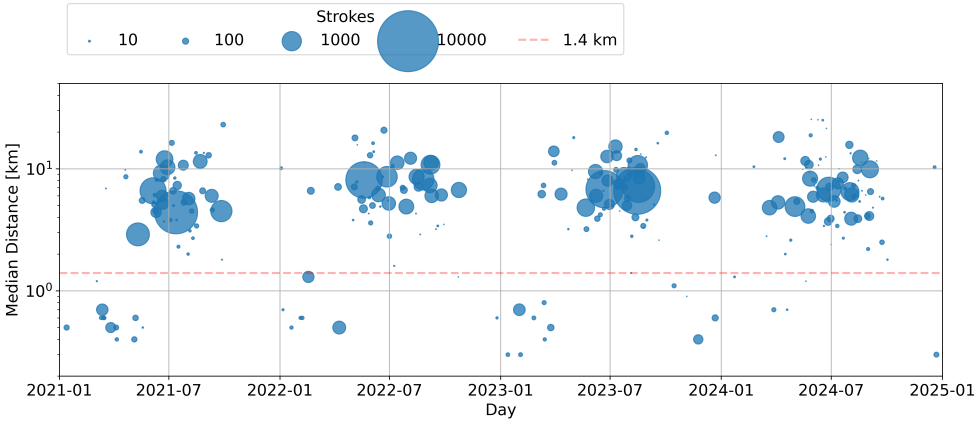

Figure 4: Daily distribution of lightning activity from winter 2021 to winter 2024. Each circle corresponds to a day with at least one detected stroke; circle diameter is proportional to stroke count. The vertical position represents the median distance to the nearest wind turbine. The dashed red line marks the estimated Blitzortung location uncertainty (≈1.4 km).

4.3. ENTLN lightning classification

ENTLN coverage in Europe is sufficient from the year 2023 onward. For cold-season Lightning Episodes in 2023, we classified Strokes into intracloud strokes (IC), negative cloud to ground strikes (CG-), and positive cloud to ground strikes (CG+). ENTLN polarity confidence threshold was set strictly to $\geq 80\%$, eliminating borderline cases.

Please note that the classification category CG- includes both negative downward cloud to ground strikes as well as negative upward (Ground to Cloud) strikes.

The classification summary is shown in Tab. 1.

4.4. Electric field

Episodes marked with an asterisk in Tab. 1 correspond to likely strikes to wind turbines within 8 km of our EFM. Radar data (ČHMÚ MAX3D;

Table 1: Cold season (November–March) Lightning Episodes in 2023 (Date). The table lists total ENTLN Strokes (Strokes), Strokes classified with given confidence ($\geq$ 80%), Intracloud Strokes (IC), negative Strikes (CG-), positive Strikes (CG+), median Blitzortung stroke distance to the nearest wind turbine in km (Median), and weather description (observer's precipitation classification / near-ground temperature) from the Karlovy Vary meteorological station (606 masl.).

Date	Strokes	$\geq$ 80%	IC	CG-	CG+	Median [km]	Weather description
2023-01-13	8	5	0	5	0	0.3	Rain / +5 ℃
2023-02-01*	35	8	1	7	0	0.7	Rain & Snow / 0 ℃
2023-03-14	21	5	0	5	0	0.8	Rain / +7 ℃
2023-03-25*	44	16	3	13	0	0.5	Rain / +7 ℃
2023-03-30	193	124	87	35	2	13.9	Rain & Snow / +11 ℃
2023-11-24*	79	37	1	36	0	0.4	Snow / +2 ℃
2023-12-21	135	55	2	51	2	5.8	Rain & Snow / +6 ℃

see Methods) were used to determine whether the same reflectivity segment passed over both the EFM and the wind turbine. Only two episodes (2023-02-01 and 2023-11-24) met this condition.

For these two episodes, we produced animations (Video 1 and Video 2) showing the evolution of the electric field (left panel) together with the corresponding radar frame (right panel). The yellow shaded region indicates the uncertainty window of the radar timestamp, because each radar image is composed of scans acquired over a period of five minutes. The spatial resolution of the MAX3D radar field is 1 km $\times$ 1 km per pixel, and the axes in the radar frames indicate horizontal coordinates in kilometres. The black line outlines the border of the Czech Republic. Red dots in the electric field plot represent the distance of lightning strokes reported by Blitzortung as seen from the EFM site. The position of the EFM itself is marked by a square symbol labelled S in the radar frames. Points labelled CH and KV denote the locations of the meteorological stations Cheb and Karlovy Vary, respectively. Plus signs indicate the positions of lightning strokes, and asterisks mark the locations of wind turbines. Strokes that occur in the vicinity of a wind turbine are highlighted in red. Radar colour shading corresponds to reflectivity in dBZ.

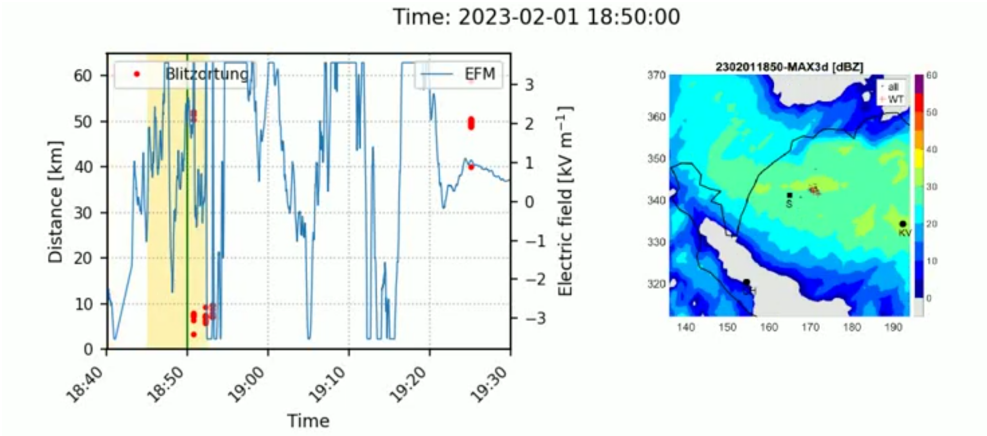

Video 1: EFM and radar data for lightning episode 1 February 2023. Animation is available here: https://youtu.be/VKD_6J6ZNBI.

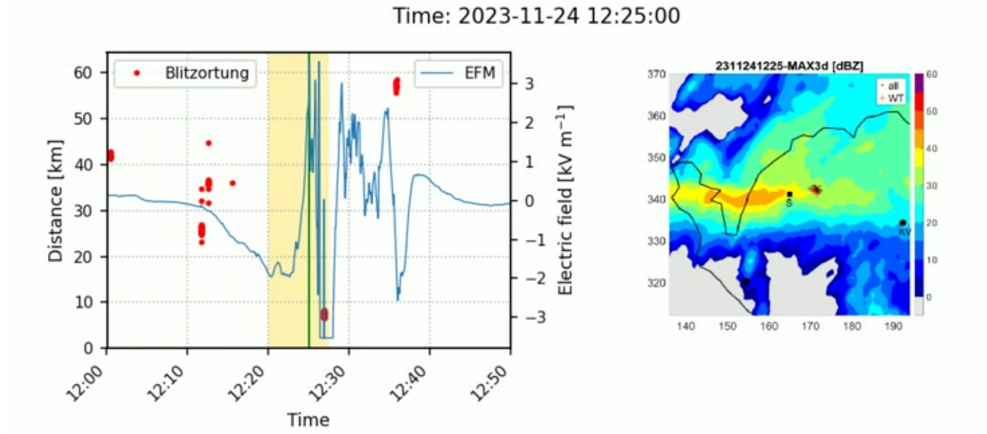

Video 2: EFM and radar data for lightning episode 24 November 2023. Animation is available here: https://youtu.be/ufh8p5zsOMg.

In both cases, the strike occurred when a region of 35–40 dBZ reflectivity passed over the wind turbine. According to EFM measurements, when such a region passed over the EFM location, the measured field was strongly negative. The absolute magnitude is unknown because the EFM range was set for summer thunderstorms, which rarely exhibit such strong ground-level electric fields.

5. Discussion

The histogram of stroke distances relative to ground structures (Fig. 3) reveals a clear dependence on the positions of wind turbines during the selected real lightning episode. To examine the seasonal behaviour of this phenomenon, we constructed Fig. 4. To distinguish individual episodes, we calculated the median distance between each stroke and the nearest wind turbine. This metric is particularly important because a lightning event may extend over a large area, and only a subset of its detected strokes may actually approach a turbine. It must also be emphasised that the Blitzortung network does not provide information on whether a given stroke is a strike. In the plots, the red dashed line marks the 1.4 km threshold, which we adopt as the approximate location accuracy of the Blitzortung system.

The figure shows that during the colder part of the year, episodes in which strokes cluster near wind turbines dominate. We therefore refer to this phenomenon as **Seasonal Wind Turbine-Associated Lightning (SWAL)**.

While Williams (2018) emphasises the importance of a lower positive charge layer (the "snow dipole") in winter storms, particularly in regimes producing energetic positive CG flashes, our observations suggest a different mode of winter electrification. In SWAL episodes, strikes polarity and near-ground electric field measurements are consistent with a dominant negative charge region exposed close to the cloud base.

For the year 2023, when accurate ENTLN data were available, we find that in all lightning episodes with a median stroke–turbine distance smaller than 1.4 km, the reported strokes were exclusively of negative polarity. This conclusion is independently supported by our EFM measurements, in which, for two episodes, we observed a pronounced negative electric field at ground level at the time when the radar-indicated reflectivity segment associated with the strike passed overhead.

During the lightning episode of 2023-02-01 (Video 1), the radar reflectivity segment that was located above the wind turbine at the moment of the lightning strike reached the EFM site several minutes later, between 18:45 and 18:55. When this segment passed over the EFM, the instrument recorded a strongly negative electric field, indicating the presence of a dominant negative charge region in the lower cloud.

During the lightning episode of 2023-11-24 (Video 2), the reflectivity segment associated with the strike passed over both the wind turbine and the EFM nearly simultaneously, between 12:20 and 12:30. At that time, the

EFM again measured a strongly negative electric field.

These observations lead to the hypothesis that under conditions associated with SWAL, the lower positive charge region of the cloud is either absent or very weak, exposing the main negative charge layer directly to the surface. Although temperatures close to 0°C would, according to laboratory-based electrification models Takahashi (1978); Saunders et al. (2006), allow the formation of such a lower positive layer, our results suggest that, during SWAL conditions, non-inductive charging in the temperature range from 0 to −10°C is either suppressed or does not occur efficiently.

Another noteworthy result is that the electric fields generated by winter clouds often reach higher magnitudes than those observed during most summer storms. This may be related to the lower cloud-base height in winter, as well as to a more monotonic charge structure with horizontally extensive charge regions near the cloud base.

For comparison, we include typical EFM records of a winter lightning episode (Fig. 5) and a summer thunderstorm (Fig. 6), both recorded with the same instrument at the same location. Both episodes produced lightning events within 8 km of the instrument, and the record duration and vertical scaling are identical.

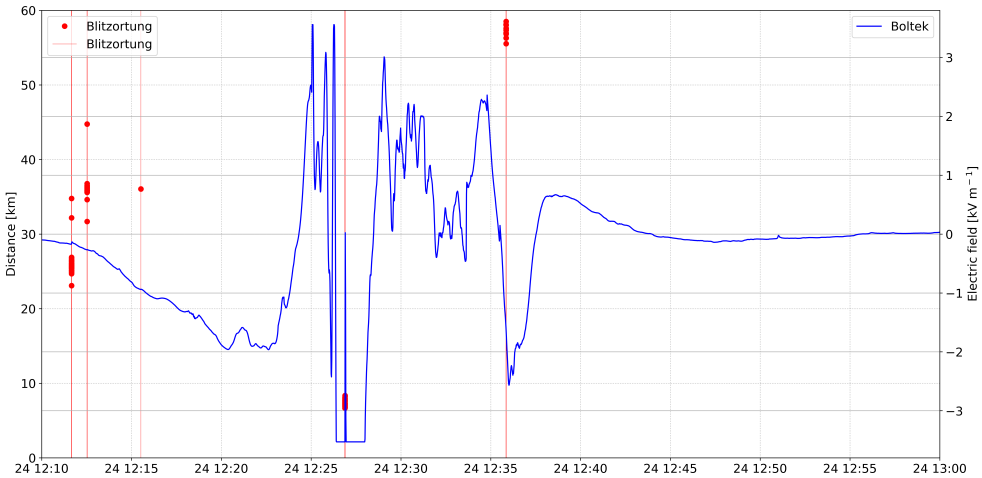

Figure 5: Electric field record during the lightning episode on 24 November 2023. Distances of the detected strokes (red dots) are given relative to the location of the EFM instrument.

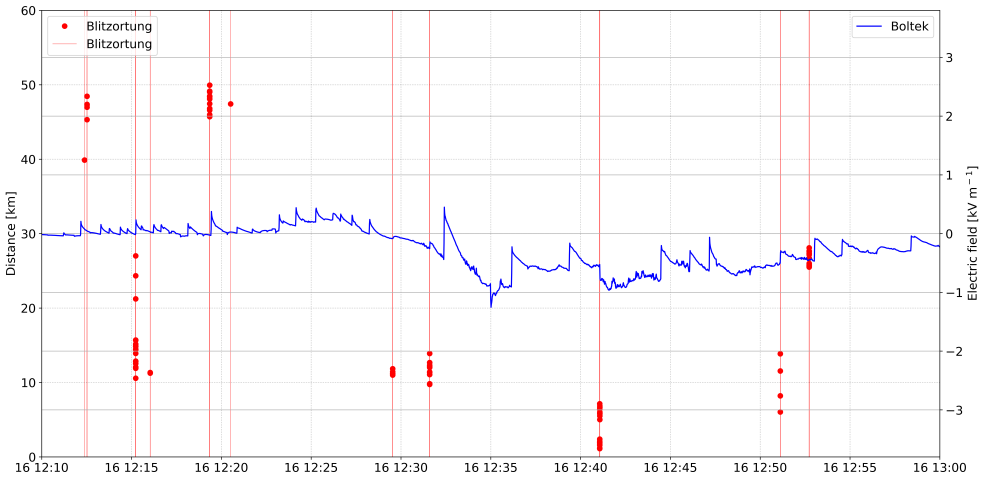

Figure 6: Electric field record during the lightning episode on 6 August 2023. Distances of the detected strokes (red dots) are given relative to the location of the EFM instrument.

Finally, we present an example of a lightning episode that produced only wind turbine-associated lightning events. If we accept the criterion that all strokes occurring within one second belong to a single lightning event, we can construct the animation (Video 3) that shows whether each lightning event contains at least one stroke approaching a wind turbine within 1.4 km. In the animation, all strokes that belong to a given lightning event (within the same one-second interval) are marked with cyan circles. If any of these strokes occur within 1.4 km of a wind turbine, that turbine is highlighted with a red dot.

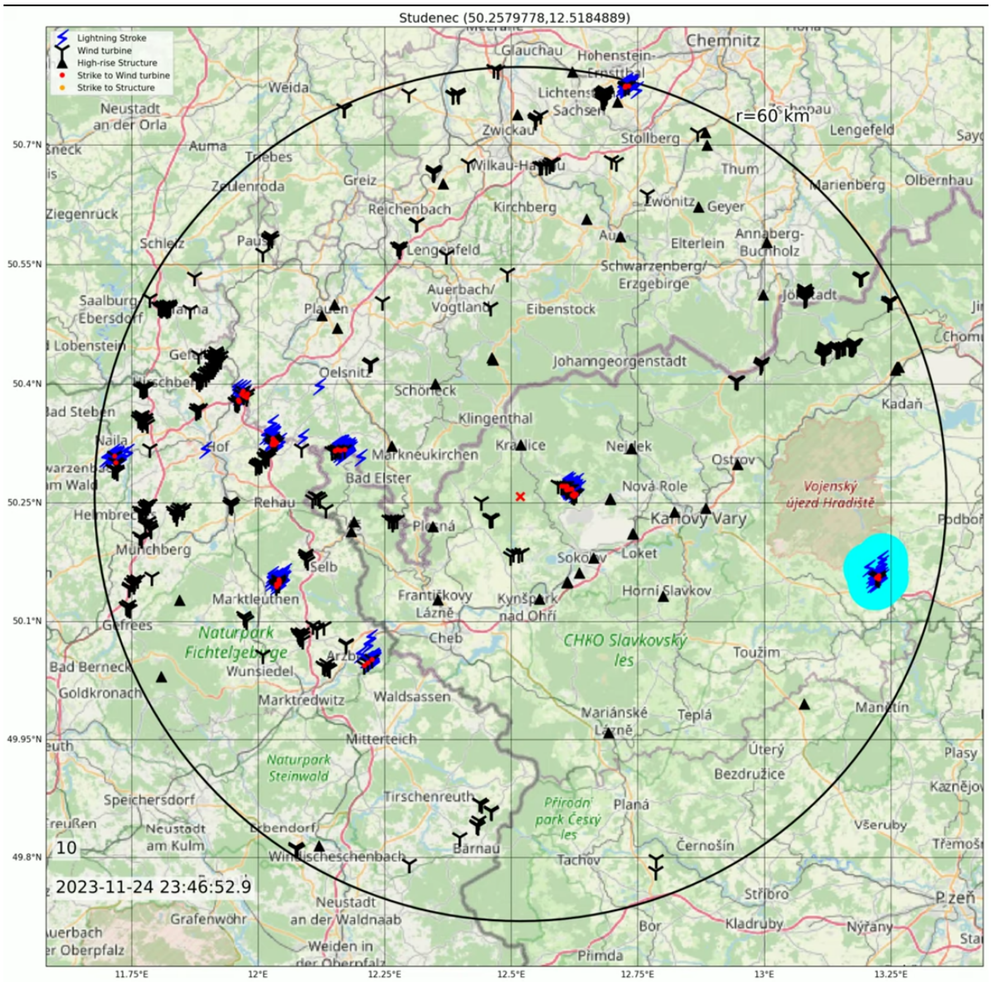

Video 3: Animation of the lightning episode on 24 November 2023. Animation is available at: https://www.youtube.com/watch?v=jIgVS3HVkIo.

6. Conclusion

This study demonstrates that cold-season lightning in Central Europe can exhibit a distinct and recurrent spatial association with wind turbines. Analysis of four years of Blitzortung stroke data, supported by ENTLN specific data and local electric field measurements, reveals that a subset of cold season Lightning Episodes is characterised by lightning activity concentrated almost exclusively within the location uncertainty of nearby wind turbines. We refer to this phenomenon as **Seasonal Wind Turbine-Associated Lightning**

(SWAL).

Episodes classified as SWAL show three consistent features: (i) their strokes occur in proximity of wind turbines, (ii) the strokes are exclusively of negative polarity, and (iii) during the events for which electric field data are available, the cloud region passing the wind turbines exhibits a strongly negative field, suggesting either the absence or strong suppression of the lower positive charge layer normally expected from non-inductive charging at temperatures near 0°C to −10°C.

These findings raise an important question: **Would SWAL-like episodes occur even without wind turbines, or do turbines modify the local electric environment in a way that enables lightning that would not otherwise develop?**

Because the documented episodes produce strikes only in the vicinity of wind turbines and do not resemble fully developed winter thunderstorms, it remains uncertain whether the meteorological conditions would have evolved into a typical winter storm in the absence of turbines. The term SWAL is therefore descriptive and does not imply a conventional winter lightning regime.

The results presented here highlight the need for high-resolution modelling and targeted observations of cold-season cloud electrification in the vicinity of large wind farms. Understanding whether SWAL is a turbine-induced phenomenon, or a naturally occurring but previously unrecognized mode of winter lightning, will be essential both for lightning physics and for the assessment of turbine-related lightning risk in Central Europe.

Acknowledgements

This work was supported by the EU Operational Programme *Research, Development and Education* (OP RDE) under the project **CRREAT – Research Centre of Cosmic Rays and Radiation Events in the Atmosphere**. The lead author, M. Kákona, was supported by the **Fulbright–Masaryk Fellowship**.

The authors gratefully acknowledge the volunteers and station operators of the **Blitzortung.org** lightning detection network for providing community accessible stroke data that made this analysis possible.

We also thank the **Earth Networks Total Lightning Network (ENTLN)** for supplying lightning classification and polarity information used in this study.

We sincerely acknowledge the global **OpenStreetMap community** for their continuous volunteer contributions that enable open, high-quality geospatial datasets. Wind turbine and infrastructure data used in this work were obtained from OpenStreetMap and are © OpenStreetMap contributors, distributed under the **Open Database License (ODbL) 1.0**.

We also acknowledge the **Czech Hydrometeorological Institute (ČHMÚ)** for providing access to radar and meteorological data, including the MAX3D reflectivity product used in this study.

References

Boltek Corporation, 2023. EFM-100 Electric Field Mill — Installation / Operator's Guide (EFM-100C). Accessed: 2024-12-01.

Candela Garolera, A., Madsen, S.F., Nissim, M., Myers, J.D., Holboell, J., 2016. Lightning damage to wind turbine blades from wind farms in the u.s. IEEE Transactions on Power Delivery 31, 1043–1049. doi:10.1109/TPWRD.2014.2370682.

Chen, H., Chen, W., Wang, Y., Xiang, N., He, T., Gu, J., Zhang, S., Sun, T., 2021. Analysis of the cloud-to-ground lightning characteristics before and after installation of the coastal and inland wind farms in china. Electric Power Systems Research 190, 106835. URL: https://www.sciencedirect.com/science/article/pii/S0378779620306350, doi:10.1016/j.epsr.2020.106835.

Haklay, M., 2010. How good is volunteered geographical information? a comparative study of openstreetmap and ordnance survey datasets. Environment and Planning B: Planning and Design 37, 682–703. URL: https://doi.org/10.1068/b35097, doi:10.1068/b35097, arXiv:https://doi.org/10.1068/b35097.

Kákona, J., Mikeš, J., Ambrožová, I., Ploc, O., Velychko, O., Sihver, L., Kákona, M., 2023. In situ ground-based mobile measurement of lightning events above central europe. Atmospheric Measurement Techniques 16, 547–561. doi:10.5194/amt-16-547-2023.

Kákona, M., et al., 2025. Lightning and wind turbine analysis scripts. https://github.com/ODZ-UJF-AV-CR/Paper-SWAL. Accessed 2025-12.

Mallick, S., Rakov, V., Hill, J., Ngin, T., Gamerota, W., Pilkey, J., Jordan, D., Uman, M., Heckman, S., Sloop, C., Liu, C., 2015. Performance characteristics of the entln evaluated using rocket-triggered lightning data. Electric Power Systems Research 118, 15–28. URL: https://www.sciencedirect.com/science/article/pii/S0378779614002168, doi:10.1016/j.epsr.2014.06.007. the Lightning Flash and Lightning Protection (SIPDA 2013).

Matsui, M., Michishita, K., Yokoyama, S., 2020. Cloud-to-ground lightning flash density and the number of lightning flashes hitting wind turbines in japan. Electric Power Systems Research 181, 106066. URL: https://www.sciencedirect.com/science/article/pii/S0378779619303852, doi:10.1016/j.epsr.2019.106066.

Montanyà, J., Fabró, F., van der Velde, O., et al., 2016. Global distribution of winter lightning: a threat to wind turbines and aircraft. Natural Hazards and Earth System Sciences 16, 1465–1472. doi:10.5194/nhess-16-1465-2016.

Montanyà, J., van der Velde, O., Williams, E.R., 2014. Lightning discharges produced by wind turbines. Journal of Geophysical Research: Atmospheres 119, 1455–1462. URL: https://agupubs.onlinelibrary.wiley.com/doi/abs/10.1002/2013JD020225, doi:10.1002/2013JD020225, arXiv:https://agupubs.onlinelibrary.wiley.com/doi/pdf/10.1002/2013JD020225.

Narita, T., Wanke, E., Sato, M., Sakanoi, T., Kumada, A., Kamogawa, M., Ishikawa, H., Harada, S., Kameda, T., Tsuchiya, F., Kaneko, E., 2018. A study of lightning location system (blitz) based on vlf sferics, in: 2018 34th International Conference on Lightning Protection (ICLP), IEEE. pp. 1–7. doi:10.1109/ICLP.2018.8503311.

OpenStreetMap contributors, 2024. Planet dump retrieved from https://planet.osm.org. https://www.openstreetmap.org. Accessed: 2025-01-01.

Overpass API Developers, 2025. Overpass turbo. URL: https://overpass-turbo.eu. accessed: 2025-01.

Rakov, V.A., Uman, M.A., 2003. Lightning: Physics and Effects. Cambridge University Press, Cambridge, UK. doi:10.1256/wea.168/03.

Saunders, C.P.R., Bax-norman, H., Emersic, C., Avila, E.E., Castellano, N.E., 2006. Laboratory studies of the effect of cloud conditions on graupel/crystal charge transfer in thunderstorm electrification. Quarterly Journal of the Royal Meteorological Society 132, 2653–2673. URL: https://rmets.onlinelibrary.wiley.com/doi/abs/10.1256/qj.05.218, doi:10.1256/qj.05.218, arXiv:https://rmets.onlinelibrary.wiley.com/doi/pdf/10.1256/qj.05.218.

Takahashi, T., 1978. Riming electrification as a charge generation mechanism in thunderstorms. Journal of the Atmospheric Sciences 35, 1536–1548. doi:10.1175/1520-0469(1978)035<1536:REAACG>2.0.CO;2.

Wanke, E., 2011. Blitzortung.org – a low-cost time of arrival lightning detection and location network (green pcb 6.6 / pcb 5.6 documentation). https://www.blitzortung.org/Compendium/Documentations/Documentation_2011-04-01_Green_PCB_6.6_PCB_5.6.pdf. Accessed: 2025-12-01.

Williams, E., 2018. Lightning activity in winter storms: A meteorological and cloud microphysical perspective. IEEJ Transactions on Power and Energy 138, 364–373. doi:10.1541/ieejpes.138.364.